Slowing Down of the Crystallization Kinetics in Ultrathin Polymer Films: A Size or an Interface Effect?

Simone Napolitano* and Michael Wübbenhorst

Katholieke Universiteit Leuven, Laboratory for Acoustics and Thermal Physics, Department of Physics and Astronomy, Celestijnenlaan 200D, B-3001 Heverlee, Belgium

Received June 12, 2006
Revised Manuscript Received July 25, 2006

The crystallization kinetics in ultrathin polymer films have been investigated by several spectroscopic techniques in both isothermal,[1−4] i.e., annealing at a temperature T_a between the glass transition temperature T_g and the melting point T_m, and nonisothermal conditions.[1−3] As a general trend, it was found that the rate of crystallization strongly decreases upon reducing the thickness, leading to an increase of the half crystallization time $t_{1/2}$ up to several orders of magnitude compared to the bulk conditions. Temperatures scans revealed that the cold crystallization temperature T_{CC}, defined as the temperature where $t_{1/2}(T)$ shows a minimum, increases with a reduction of the thickness of the polymer layer. The thinnest films are thus characterized by a higher glass stability,[5] and in particular conditions the crystallization is inhibited.[6] Several theoretical models[7−9] predicted an anomalous behavior of the crystallization kinetics due to the reduction of both the crystal nucleation and growth rate in thin films. In particular, it was suggested that systematic deviations from the Avrami law are generated when the ratio between the sample thickness a and the linear growth rate, g, deviates from an infinite value.[7] Thus, variations of the Avrami coefficients in ultrathin films cannot be directly attributed to a reduction of dimensionality of the crystallization process itself.

Imaging techniques were able to detect morphological changes in the structure[10−17] and made it possible to measure directly the linear crystal growth rate, that in films of a few nanometer drops to values down to 1% of those characteristic of the bulk.[10] For PEO the ratio a/g was found to vary from 75 for bulk films to 0.04 for the thinnest films.

Again for PEO, it was proposed[10] that the slowing down affecting the crystallization kinetics in the thinnest films is due both to a confinement effect and an interface: it was argued that the reduction of the crystal growth factor by 2 orders of magnitude was imputable to an increase of 30 °C in the glass transition temperature due to a highly interacting substrate. To discriminate between size, deviations of dynamical properties from the bulk value in proximity of a characteristic length scale of system (like for the glass transition temperature and the gyration radius), and interface effects, i.e., changes of chain mobility in a region governed by the long-range effects of the interfacial interaction, it is necessary to use techniques that can both access the glass transition temperature and monitor the crystallization kinetics in nanometer-thick polymer films.

In this Communication we present the first experimental work on monitoring in real time the cold crystallization kinetics of ultrathin polymer films via broadband dielectric spectroscopy (DS). This technique has already been successfully used to detect and study relaxation processes in ultrathin polymer films. Even on the nanometer scale, DS provides, in fact, not only several sensitive experimental methodologies to assign the glass transition temperature[18−20] but also the possibility of accessing a broadband frequencies scenario of the changes induced by geometrical constraint and confinement to the segmental mobility, local secondary relaxations,[21,22] and the relaxation of the whole chain, namely normal mode.[23]

The technique itself has been widely used to monitor crystallization kinetics of both polar[24−41] and nonpolar[42] polymer chains in bulk, being a sensitive tool to investigate the dynamic changes during the crystals' growth in terms of reduction of the mobility (shift of the structural relaxation toward lower frequency) and the volume fraction (decrease of the relaxation strength $\Delta\epsilon_\alpha$) of the amorphous phase.

To prove the feasibility of DS as an experimental approach to investigate crystallization in ultrathin polymer films, poly(3-hydroxybutyrate), PHB, a polar biodegradable polyester showing a simple dielectric scenario, has been chosen as sample material. At room temperature, in fact, the polymer shows a strong peak corresponding to the structural relaxation, often referred as α and connected to the segmental motion; a weak β-relaxation, probably due to the ester group present in the main chain,[36] is present at higher frequencies outside the typical measurement range. Moreover, considering the high flexibility of the polymer chain, the α-peak maximum, f_{max}, correlated to the most probable (as a maximum in distribution function) relaxation time of the process τ_α by the simple relation $2\pi\tau_\alpha f_{max} \approx 1$, is not affected by crystallization;[25,36] for other semicrystalline polyesters with less flexible chains like PET,[24,32] PEN,[38] and PEEK,[35] a shift toward lower frequencies is observed, an indication of a reduction in the segmental mobility connected to an increase of the glass transition temperature during the crystallization itself. These unique features make PHB an attractive model system for crystallization studies monitored by DS.

The crystallization kinetics of PHB have been monitored in both bulk and ultrathin amorphous samples. By a detailed analysis of the spectra recorded, it was possible to distinguish the nature of the deviation from bulk behavior.

Bulk amorphous samples were produced by cooling a molten polymer layer obtained by holding the polymer powder (M_w = 170K, by Sigma) for 3 min at 175 °C (T_m^{DSC} = 160 °C). The layer was prepared between two brass circular electrodes, separated by glassy fibers (diameter = 50 μm), to avoid shortcuts. The quenching procedure was ensured by a rapid cooling of the obtained polymer sandwich between two cold plates, kept at −5 °C. A clear peak, attributed to the α-relaxation, was present in the dielectric spectra in the temperature and the frequency range as previously reported for amorphous samples of this polymer.[25,36] Ultrathin films of poly(3-hydroxybutyrate) were obtained at room temperature, thus in the region of temperature above the glass transition temperature (T_g^{DSC} = 2 °C). Solutions of the polymer were spin-coated on cleaned glass slides, onto which an aluminum strip, used as a lower electrode, was previously thermally evaporated in an ultrahigh-vacuum chamber. Samples as prepared were kept for 2 h at 45 °C in order to remove any solvent residuals. A second strip of Al was finally deposited onto the polymer surface, following the procedure described above. Film thicknesses were evaluated from the electrical capacity of the sample.[18,19]

After the applied annealing procedure the ultrathin samples were partially crystalline as indicated by dielectric spectroscopy,

* Corresponding author. E-mail: simone.napolitano@fys.kuleuven.be.

10.1021/ma061304u CCC: $33.50
Published on Web 08/10/2006

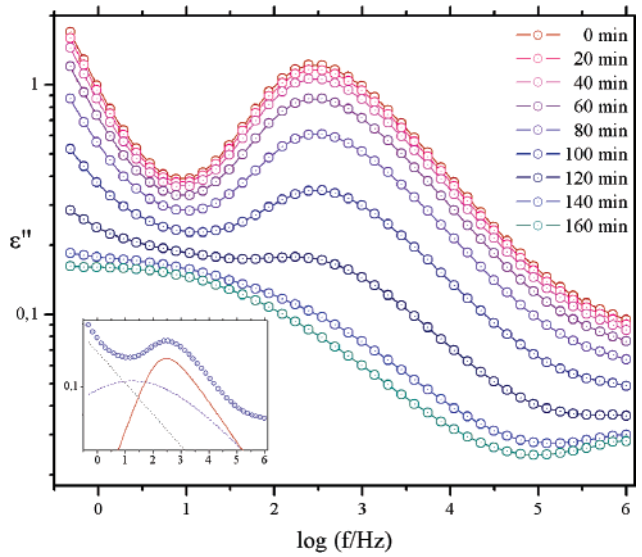

Figure 1. Dielectric spectra of a 50 μm thick sample during an isothermal crystallization at 18 °C. The continuous lines are guides for the eye. In the inset a fit for the spectrum recorded after 105 min of annealing. The spectrum was deconvolved as sum of a conductive contribute and two relaxation processes as referred in the text: the structural relaxation and the constrained amorphous phase at lower frequencies.

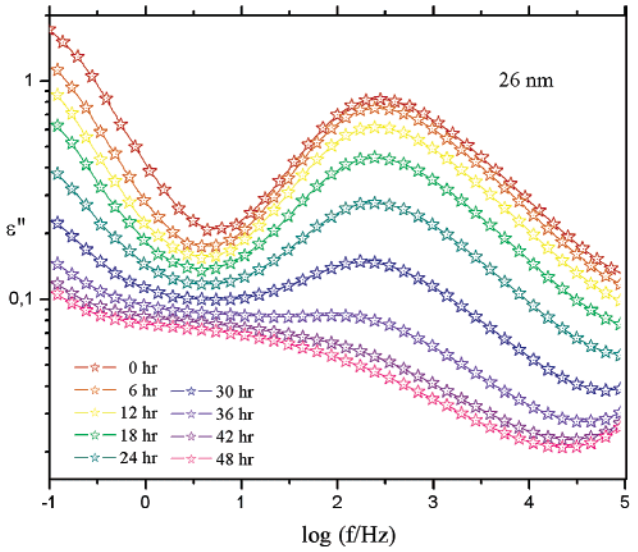

Figure 2. Dielectric spectra of a 26 nm thick sample during an isothermal crystallization at 18 °C. The continuous lines are guides for the eye.

i.e., the α-relaxation was not detected. To obtain amorphous samples, the polymer layers were melted and quenched as reported above for bulk samples. Successful amorphizations resulted in samples showing an α-relaxation peaked in the same frequency range and with a similar intensity as observed for bulk samples. (For the thinnest films analyzed, the dielectric strength was reduced of 10% compared to the bulk value, as discussed below.)

Dielectric spectra were recorded with an high-resolution analyzer (ALPHA-A from Novocontrol Technologies) immediately after amorphization. Storing the samples at room temperature ($T_{amb} > T_g$) in fact would favor nucleation. In a similar way, even in the case of moderate annealing procedures above T_g, necessary to remove the solvent, uncontrolled nucleation phenomena leading to faster crystallization kinetics could take place. A more detailed explanation of this question will be addressed in a separate paper.

Spectra of the complex dielectric permittivity, $\epsilon^*(\omega) = \epsilon'(\omega) - i\epsilon''(\omega)$, were recorded under a continuous nitrogen flow in isothermal conditions with a temperature stability better than 0.1 °C. The low-frequency limit (1.2 Hz for bulk samples and 0.49 Hz for the thinnest film) was chosen to reach real-time conditions; i.e., the process monitored has a mean time much larger than the measurement time so that each single spectrum can be considered as a snapshot of the process itself.

Figure 1 and Figure 2 show respectively the time evolution of the isothermal crystallization of a bulk sample (50 μm at 18 °C) and a ultrathin film (26 nm at 18 °C) as monitored by DS. In both samples the same features are recognized. After an induction time during which the spectra show no changes from the one recorded for the amorphous sample, the dielectric strength of the structural relaxation $\Delta\epsilon_\alpha$ decreases, leading to a reduction of the height of the α-peak. A reduction of $\Delta\epsilon$ corresponds to a decrease of the density of the fluctuating dipoles, giving rise to the dielectric signal: the dipoles of crystallized part of the samples, being immobilized, do not contribute to the recorded signal.

As previously indicated for other polymers,[32,35] in the advanced stages of crystallization, a second weaker peak was detected at the low-frequency side of the α-relaxation. This peak, often referred as α′, shows an increase of the intensity during the drop in $\Delta\epsilon_\alpha$, indicating that a change is occurring in the polymer fraction that contributes to the α-relaxation. The molecular origin of α′ could be related to the relaxation of the amorphous fraction constrained within the growing lamellae. This confined phase shows, in fact, a lower mobility compared to the one characterizing the free amorphous phase. The crystallization of these regions corresponds to the secondary crystallization that can be thus monitored by following the further evolution of $\Delta\epsilon_{\alpha'}$.

The ratio between the intensity of the constrained amorphous phase (α′-peak) and the structural relaxation (α-peak), $\phi(\alpha'/\alpha) \equiv \epsilon''_{\alpha'}{}^{max}/\ \epsilon''_{\alpha}{}^{max}$, is relatively low compared to the values recorded for other polyesters, i.e., $\phi(\alpha'/\alpha) \approx 0.1$ for PHB and ≈ 0.4 for PET.[24] Coupling such a low value with the non-influence of the crystals' growth on the f_{max} recorded for the structural relaxation (likewise for bulk samples even in ultrathin films f_{max} is constant within the crystallization time), it can be argued that in the temperature range investigated the reduction of the amorphous volume fraction can be directly correlated to the increase of crystalline content in this system. This trend has already been observed for low molecular weight molecules[39] and is a signature of non-strongly-interfering coexisting phases characterized by a different crystalline content. Such a model matches a semicrystalline polymer with flexible chains as PHB well.

As previously stated, spectra of less flexible polymers are characterized by a shift of the α-relaxation toward lower frequencies and higher values for $\phi(\alpha'/\alpha)$. These features indicate that the drop in the dielectric signal is due not only to a reduction of the amorphous phase but also to a strong immobilization of the amorphous chains at the very interface with the crystals, due to the formation to the so-called rigid amorphous fraction, RAF, the region at the interface between the immobilized crystalline chains and the mobile amorphous phase showing intermediate properties between the two.[43−46] In similar systems it was found that the time scale of the process observed by X-rays scattering is however of the same order of magnitude of the one reported by DS,[32] being usually $t_{1/2}{}^{XRS} \approx 2t_{1/2}{}^{DS}$.

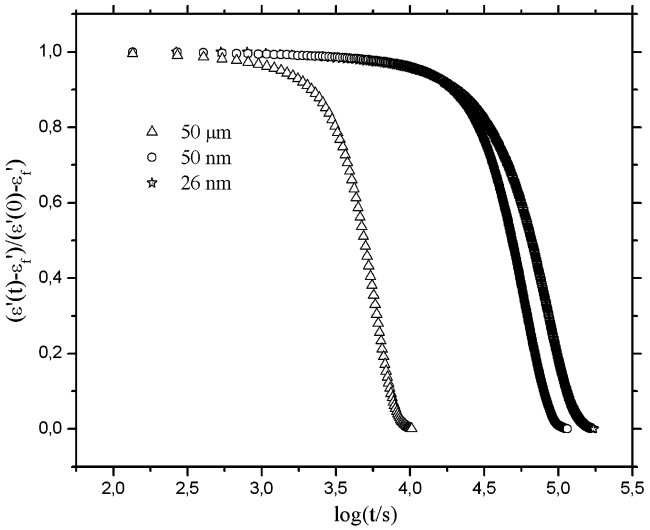

Figure 3. Time evolution of the normalized dielectric constant at 10 Hz for the analyzed samples. ϵ'_f is the lower value of the dielectric constant during the primary crystallization. The half crystallization time $t_{1/2}$ is given by the midpoint of the step in the curve.

For PHB, as the crystallization affects the spectra of both ultrathin films and bulk samples similarly, the reduction of sample thickness does not interfere with the changes occurring in the amorphous fraction during the crystallites' formation. The only difference between macroscopic and nanometer-thick samples is a tremendous change in the time scale of the event. The half crystallization time, as estimated by DS in terms of the midpoint in the step shown in the normalized dielectric constant[47] (see Figure 3), increases by an order of magnitude for the thinnest films, $t_{1/2}(26\text{ nm}) \approx 14t_{1/2}(\infty)$. The result accords with the values already reported for other systems using different investigation techniques.[10,48]

To prove whether such an increase of $t_{1/2}$ could be correlated to an increase of T_g, we monitored the thermal evolution of the α-relaxation of amorphous samples (ultrathin films were spin-coated from the same solutions used for the films to be crystallized) to extract the values of the relative dynamic glass transition temperatures. The data collected were analyzed in terms of a Vogel−Fulcher−Tamman (VFT) equation:

$$\tau_{max}(T) = \tau_\infty \exp\left(-\frac{B}{T - T_0}\right) \quad (1)$$

where T_0 if the Vogel temperature, B is a parameter related to the curvature of $\tau_{max}(T)$, and τ_∞ is the relaxation time in the limit of infinite temperatures. The dynamic glass transition temperature was obtained by extrapolating the experimental curves toward the temperature at which the structural relaxation is characterized by a relaxation time of 100 s. The results, shown in Figure 4, show that no dependence of the thermal evolution of τ_{max} on the thickness of the sample was found down to 26 nm; i.e., similar to other polymers,[18,19,49] the segmental mobility of PHB does not feel the effects of confinement. It is then not possible to attribute the increase of the crystallization time to a reduction of the chain mobility on the time and the length scale of the dynamic glass transition. Furthermore, FTIR measurements[3] showed that for PET an increase of $\tau_{1/2}$ is combined with a reduction of T_g.[50] The glass transition temperature averaged over the thickness of the whole film does not seem to be a good parameter to describe the influence of chain mobility on the crystallization kinetics.

A more accurate analysis of the spectra revealed a reduction of the dielectric strength of the α-process, a systematic change

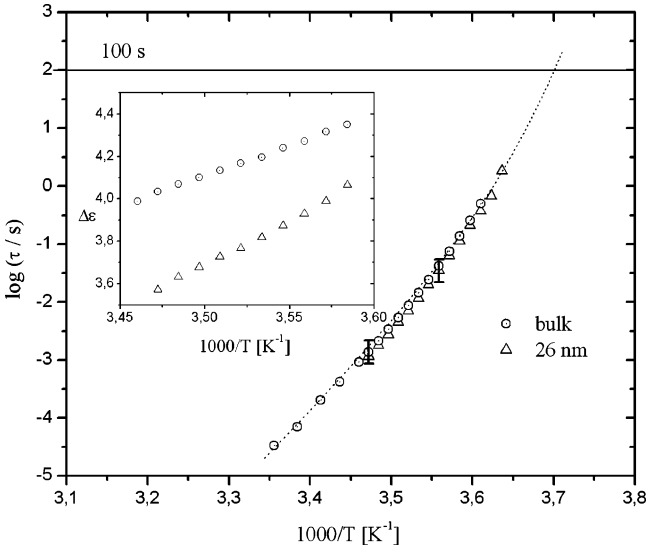

Figure 4. Thermal evolution of the most probable relaxation time (maximum of the time distribution) for the structural process of the thinner and the thickest sample. The same VFT curve can be used to fit both series of data. Down to 26 nm, T_g, indicated in the figure as the temperature at which the structural relaxation last 100 s, shows no thickness dependence.

already reported in other polymer systems[18,19] usually attributed to the presence of low-mobility region, often referred to as dead layer, giving rise to a reduced dielectric signal (the dielectric strength dropped by 10% compared to the bulk value; see inset of Figure 4). For PHB it was recently argued that the increase of crystallization time could be due to a reduction in mobility of the chain segments at the very interface with the substrate[6] that corresponds to the dead layer detected by a reduction of $\Delta\epsilon$ in the dielectric spectra. Qualitatively similar results were found for other systems:[3] the interaction between the substrate and the film plays a role in the crystallization kinetics; the stronger the interaction, the more the chain mobility is reduced and the bigger is $t_{1/2}$.

The reduced mobility of the chains at the interface could in fact inhibit the material transport[12] and consequently induce a slowing down in the crystallization kinetics. A similar mechanism is confirmed by a very recent dynamic Monte Carlo simulation:[9] in the case of sticky walls, due to a restriction of polymer motions within the chains at the very interface, the crystallization is frustrated.

Dielectric spectroscopy was successfully employed to monitor in real time the crystallization kinetics of ultrathin polymer films of PHB. It was observed that the thickness of the sample does not influence the changes occurring in the amorphous phase due to crystallization. Moreover, as the technique was able to access the dynamic glass transition temperature even on the nanometer scale, it was possible to discriminate between the influence of T_g and the reduction of mobility of the polymer layers at the very interface with the substrate on the drastic changes in the crystallization kinetics. This last factor seems to play a fundamental role and drives the tremendous slowing down observed in the crystallization kinetics of ultrathin polymer films.

Acknowledgment. S.N. acknowledges financial support from the European Community's "Marie-Curie Actions" under Contract MRTN-CT-2004-504052 [POLYFILM] and Mrs. V. Lupaşcu and Mr. P. Droppert for their friendly help during sample preparation.

CDV

References and Notes

(1) Despotopoulou, M. M.; Miller, R. D.; Rabolt, J. F.; Frank, C. W. *J. Polym. Sci., Part B: Polym. Phys.* **1996**, *34*, 2335−2349.
(2) Despotopoulou, M. M.; Frank, C. W.; Miller, R. D.; Rabolt, J. F. *Macromolecules* **1996**, *29*, 5797−5804.
(3) Zhang, Y.; Lu, Y. L.; Duan, Y. X.; Zhang, J. M.; Yan, S. K.; Shen, D. Y. *J. Polym. Sci., Part B: Polym. Phys.* **2004**, *42*, 4440−4447.
(4) Zhang, Y.; Mukoyama, S.; Mori, K.; Shen, D. Y.; Yan, S. K.; Ozaki, Y.; Takahashi, I. *Surf. Sci.* **2006**, *600*, 1559−1564.
(5) Nascimento, M. L. F.; Souza, L. A.; Ferreira, E. B.; Zanotto, E. D. *J. Non-Cryst. Solids* **2005**, *351*, 3296−3308.
(6) Capitan, M. J.; Rueda, D. R.; Ezquerra, T. A. *Macromolecules* **2004**, *37*, 5653−5659.
(7) Schultz, J. M. *Macromolecules* **1996**, *29*, 3022−3024.
(8) Sommer, J. U.; Reiter, G. *Thermochim. Acta* **2005**, *432*, 135−147.
(9) Ma, Y.; Hu, W.; Reiter, G. *Macromolecules* **2006**, *39*, 5159−5164.
(10) Schonherr, H.; Frank, C. W. *Macromolecules* **2003**, *36*, 1199−1208.
(11) Schonherr, H.; Frank, C. W. *Macromolecules* **2003**, *36*, 1188−1198.
(12) Massa, M. V.; Dalnoki-Veress, K.; Forrest, J. A. *Eur. Phys. J. E* **2003**, *11*, 191−198.
(13) Massa, M. V.; Dalnoki-Veress, K. *Phys. Rev. Lett.* **2004**, *92*.
(14) Massa, M. V.; Carvalho, J. L.; Dalnoki-Veress, K. *Eur. Phys. J. E* **2003**, *12*, 111−117.
(15) Taguchi, K.; Miyaji, H.; Izumi, K.; Hoshino, A.; Miyamoto, Y.; Kokawa, R. *J. Macromol. Sci., Phys.* **2002**, *B41*, 1033−1042.
(16) Gan, Z. H.; Abe, H.; Doi, Y. *Biomacromolecules* **2000**, *1*, 713−720.
(17) Huang, Y.; Liu, X. B.; Zhang, H. L.; Zhu, D. S.; Sun, Y. J.; Yan, S. K.; Wang, J.; Chen, X. F.; Wan, X. H.; Chen, E. Q.; Zhou, Q. F. *Polymer* **2006**, *47*, 1217−1225.
(18) Lupascu, V.; Huth, H.; Schick, C.; Wübbenhorst, M. *Thermochim. Acta* **2005**, *432*, 222−228.
(19) Fukao, K.; Miyamoto, Y. *Phys. Rev. E* **2000**, *61*, 1743−1754.
(20) Fukao, K.; Miyamoto, Y. *J. Phys., IV* **2000**, *10*, 243−246.
(21) Fukao, K.; Uno, S.; Miyamoto, Y.; Hoshino, A.; Miyaji, H. *Phys. Rev. E* **2001**, *6405*.
(22) Wübbenhorst, M.; Lupascu, V. In *ISE-12*; IEEE: Brazil, 2005; pp 87−90.
(23) Serghei, A.; Kremer, F. *Phys. Rev. Lett.* **2003**, *91*.
(24) Alvarez, C.; Sics, I.; Nogales, A.; Denchev, Z.; Funari, S. S.; Ezquerra, T. A. *Polymer* **2004**, *45*, 3953−3959.
(25) Bergmann, A.; Owen, A. *Polym. Int.* **2004**, *53*, 863−868.
(26) El Shafee, E. *Eur. Polym. J.* **2001**, *37*, 451−458.
(27) Ezquerra, T. A.; Liu, F.; Boyd, R. H.; Hsiao, B. S. *Polymer* **1997**, *38*, 5793−5800.
(28) Ezquerra, T. A.; Majszczyk, J.; Baltacalleja, F. J.; Lopezcabarcos, E.; Gardner, K. H.; Hsiao, B. S. *Phys. Scr.* **1994**, *55*, 212−215.
(29) Ezquerra, T. A.; Sics, I.; Nogales, A.; Denchev, Z.; Balta-Calleja, F. J. *Europhys. Lett.* **2002**, *59*, 417−422.
(30) Fukao, K.; Miyamoto, Y. *Prog. Theor. Phys. Suppl.* **1997**, 219−222.
(31) Fukao, K.; Miyamoto, Y. *J. Non-Cryst. Solids* **1997**, *212*, 208−214.
(32) Fukao, K.; Miyamoto, Y. *J. Non-Cryst. Solids* **1998**, *235*, 534−538.
(33) Jimenez-Ruiz, M.; Ezquerra, T. A.; Sics, I.; Fernandez-Diaz, M. T. *Appl. Phys. A:* **2002**, *74*, S543−S545.
(34) Mansour, A. A.; Saad, G. R.; Hamed, A. H. *Polymer* **1999**, *40*, 5377−5391.
(35) Nogales, A.; Ezquerra, T. A.; Denchev, Z.; Sics, I.; Calleja, F. J. B.; Hsiao, B. S. *J. Chem. Phys.* **2001**, *115*, 3804−3813.
(36) Nogales, A.; Ezquerra, T. A.; Garcia, J. M.; Balta-Calleja, F. J. *J. Polym. Sci., Part B: Polym. Phys.* **1999**, *37*, 37−49.
(37) Sanz, A.; Nogales, A.; Ezquerra, T. A.; Lotti, N.; Munari, A.; Funari, S. S. *Polymer* **2006**, *47*, 1281−1290.
(38) Nogales, A.; Denchev, Z.; Sics, I.; Ezquerra, T. A. *Macromolecules* **2000**, *33*, 9367−9375.
(39) Alie, J.; Menegotto, J.; Cardon, P.; Duplaa, H.; Caron, A.; Lacabanne, C.; Bauer, M. *J. Pharm. Sci.* **2004**, *93*, 218−233.
(40) Wurm, A.; Soliman, R.; Schick, C. *Polymer* **2003**, *44*, 7467−7476.
(41) Wurm, A.; Soliman, R.; Goossens, J. G. P.; Bras, W.; Schick, C. *J. Non-Cryst. Solids* **2005**, *351*, 2773−2779.
(42) van den Berg, O.; Sengers, W. G. F.; Jager, W. F.; Picken, S. J.; Wubbenhorst, M. *Macromolecules* **2004**, *37*, 2460−2470.
(43) Boyer, R. F. *Macromolecules* **1973**, *6*, 288−299.
(44) Schick, C.; Wurm, A.; Mohammed, A. *Thermochim. Acta* **2003**, *396*, 119−132.
(45) Schick, C.; Wurm, A.; Mohamed, A. *Colloid Polym. Sci.* **2001**, *279*, 800−806.
(46) Alsleben, M.; Schick, C. *Thermochim. Acta* **1994**, *238*, 203−227.
(47) Damore, A.; Kenny, J. M.; Nicolais, L.; Tucci, V. *Polym. Eng. Sci.* **1990**, *30*, 314−320.
(48) Dalnoki-Veress, K.; Forrest, J. A.; Massa, M. V.; Pratt, A.; Williams, A. *J. Polym. Sci., Part B: Polym. Phys.* **2001**, *39*, 2615−2621.
(49) Serghei, A.; Mikhailova, Y.; Huth, H.; Schick, C.; Eichhorn, K. J.; Voit, B.; Kremer, F. *Eur. Phys. J. E* **2005**, *17*, 199−202.
(50) Zhang, Y.; Zhang, J. M.; Lu, Y. L.; Duan, Y. X.; Yan, S. K.; Shen, D. Y. *Macromolecules* **2004**, *37*, 2532−2537.

MA061304U